

## Supplementary Methods

### *Generation of G6b-B diY/F mice*

A constitutive *knock-in (KI)* strategy was used to generate *G6b-B diY/F KI* mice (Figure S1). A targeting vector containing the mutated *G6b* gene and a *puromycin resistance cassette (PuroR)* flanked with flippase recognition target (FRT) sites was produced. Point mutations were inserted into the *G6b* gene, converting the tyrosine codons TAC and TAT of exon 6 (positions 648 and 726 within the transcript nucleotide sequence, taken from NM\_001191012.1) to TTC, the codon for phenylalanine. Neighboring genes were also cloned into the targeting vector, providing 7 kb and 4 kb homology arms. These allow for insertion of the mutant gene, via homologous recombination, into germline competent C57Bl6/NTac embryonic stem cells. This effectively knocks out the *WT G6b* gene and replaces it with the mutant gene, called *G6b-B diY/F*. Recombined mutants with the correctly inserted mutant construct were isolated using the *PuroR* gene positive- and thymidine kinase negative-selection. Following validation, clones were injected into mouse blastocysts and transferred into pseudopregnant female mice. *G6b-B diY/F* mice were subsequently crossed with Tg(CAG-flpe) Flp recombinase expressing mice, causing excision of the FRT sites, therefore removing the *PuroR* cassette and generating the final *G6b-B diY/F* constitutive *KI* mouse allele. Further crossing with C57Bl6/NTac mice and selective breeding removed expression of Flp recombinase in animals used for experiments.

Successful targeted *KI* was shown by PCR using oligos 1 & 2 and 5 & 6.

The residual FRT site following excision of the *PuroR* gene allows for the *WT* and *KI* alleles to be distinguished by PCR. Primers were generated to target the annealing sites indicated by oligos 3 and 4 (Figure 3.1Aiv). These produce a PCR product of

315 base pairs (bp) for the *WT* allele and 401 bp for the KI allele, which can be distinguished by running the PCR.

#### *Mouse G6b-specific antibodies*

The anti-mouse monoclonal antibody was raised by injection of Fc-fused G6b-B ectodomain into rats. As such, this antibody will recognize both G6b-A-like and G6b-B isoforms on the surface of platelets. Anti-mouse G6b-B polyclonal antibody was generated by injection of a peptide specific to G6b-B into rabbits. These were generated as previously described.<sup>1</sup>

#### *Platelet clearance*

Mice were injected intravenously with 600  $\mu$ g of N-hydroxysuccinimidobiotin (NHS)-Biotin in PBS. Blood samples were collected from tail veins, into 5 mM EDTA, 10% fetal bovine serum in PBS, at the following time points following injection: 1 hour (h) (Day 1), 24h (Day 2), 48h (Day 3), 72h (Day 4) and 96h (Day 5). Percentage of biotin positive platelets was measured by flow cytometry using PE-Streptavidin (BD Pharmingen, Oxford, UK).

#### *Platelet recovery*

Platelets were depleted by intraperitoneal (I.P.) injection of 1.5  $\mu$ g anti-GPIIb $\alpha$  antibody (Emfret Analytics, Wurzburg, Germany) per gram of mouse body weight. Blood samples were collected from the tail vein into 20 mM EDTA in PBS before I.P. injection (Day 0) and at 24 hour intervals following this. Platelet counts were measured using an ABX Pentra 60 hematological counter (Horiba Medical, Northampton, UK).

### *Platelet clearance and recovery analysis*

Proportionate slopes were calculated for each mouse using data from days one to five and days two to seven for platelet clearance and recovery assays, respectively. These slopes were taken as a measurement of rate of platelet clearance (% of platelets per day) and rate of platelet production ( $\times 10^8/\text{mL}$  platelets per day).

### *Immunohistochemistry*

Spleens and femurs from *G6b-B<sup>dY/F</sup>* and *WT* mice were fixed in buffered formalin and embedded in paraffin. Sections were H&E and reticulin stained and examined by light microscopy with a Zeiss Axio ScanZ1 (Carl Zeiss Ltd, Cambridge, UK).

### *Tail bleeding assay*

Mice were anaesthetized using isoflurane and placed on a raised heating pad at 37°C. 5 mm of the tail tip was excised using a scalpel blade and blood drops collected (falling in air) to a maximum time of 20 minutes, or 5 minutes with no blood drop falling. Bleeding tendency was quantified by determining the mass of blood loss (mg) following injury and dividing by the weight of the mouse (g). A maximum allowed blood loss was calculated for each mouse equal to  $\leq 10\%$  of body weight. Blood loss for all animals remained within this limit. Where the blood loss was recorded as zero ( $n=1$ ) a value equal to the average of zero and 50% of the limit of detection (0.1 mg blood loss) was employed.

Blood loss (mg/g) was modelled as a bi-modal function, comprising of a gamma distribution representing a low (normal) bleeding tendency and a normal distribution representing increased bleeding. The probability that a mouse of a specified genotype had a normal bleeding time was  $P_{\text{norm}}$  or was a bleeder was  $(1 - P_{\text{norm}})$ . Probabilities were modelled as logits. ( $\text{logit}(P) = \ln(P/(1-P))$ )

The maximum likelihood ( $-2LL = -2 \times \log \text{likelihood}$ ) was determined generating parameters that defined normal and increased bleeding and the logits of the probabilities of each genotype having normal bleeding. Likelihood ratio tests were performed to determine whether the probability of bleeding differed between genotypes.

Modelling was done in Microsoft Excel (Redmond, WA, USA) and replicated in NONMEM 7.3 (Icon PLC, Dublin, Ireland) to generate standard error values for the parameters.

### *Flow cytometry*

Mice were CO<sub>2</sub>-asphyxiated and blood collected from the vena cava into 1/10 (v/v) acid-citrate-dextrose anticoagulant. Fluorescein isothiocyanate (FITC)-conjugated antibodies were used to measure surface receptor expression in whole blood with an Accuri C6 flow cytometer (BD Biosciences, Oxford, UK). Values for relevant IgG controls have been subtracted from all presented data. For flow cytometry based activation assays, whole blood or  $2 \times 10^7/\text{mL}$  washed platelets were stained with FITC-conjugated P-selectin antibody or Alexa488-conjugated fibrinogen in the absence (basal) and presence of indicated agonists. Thrombin stimulations were performed in the presence of 10  $\mu\text{M}$  GPRP to prevent fibrin polymerization. For all flow cytometry 10,000 events were collected and data is presented as median fluorescence intensity. Reactions were terminated with cold 1% paraformaldehyde in PBS. The proportion of reticulated platelets in whole blood was quantified by flow cytometry following 30 minute incubation with BD Retic-Count solution (BD Biosciences, Oxford, UK).

### *Platelet adhesion and spreading on fibrinogen*

Washed platelets ( $2 \times 10^7/\text{mL}$ ) were prepared as previously described in modified Tyrodes buffer (134 mM NaCl, 2.9 mM KCl, 340  $\mu\text{M}$   $\text{Na}_2\text{HPO}_4 \cdot 12\text{H}_2\text{O}$ , 12 mM  $\text{NaHCO}_3$ , 20 mM HEPES, 1 mM  $\text{MgCl}_2$ , 5 mM glucose, pH 7.3, 37°C).<sup>2</sup> Platelet spreading assay on fibrinogen-coated coverslips was performed as previously described.<sup>3</sup> All slides were imaged using a Zeiss Axiovert 200M microscope and quantified using ImageJ. Stages of platelet spreading were categorized as unspread, formation of filopodia, formation of lamellipodia and fully spread (Figure S6).

### *Platelet aggregation and secretion*

Platelet aggregation and adenosine triphosphate (ATP) secretion was measured in washed platelets ( $2 \times 10^8/\text{mL}$ ) using a Chrono-Log Model 700 lumi-aggregometer (Havertown, PA, USA), as previously described.<sup>4</sup> ADP-sensitive platelets were prepared as previously described,<sup>5</sup> using modified Tyrodes buffer supplemented with 0.02 U/mL apyrase for washing steps. The final platelet pellet was resuspended in modified Tyrodes buffer without apyrase and before starting aggregations 1  $\mu\text{M}$   $\text{CaCl}_2$  and 50  $\mu\text{g}/\text{mL}$  fibrinogen was added to the diluted platelets. Aggregation traces were exported and mean traces calculated.

### *Platelet flow adhesion coverslip preparation*

Glass coverslips (24 × 60 mm) were coated with three microspots (0.5  $\mu\text{L}/\text{spot}$ ), which produce thrombi via different platelet-adhesive receptors (De Witt, Nat Comm 2014). The microspot coatings contained (in the direction of flow): (i) von Willebrand factor-binding peptide (VWF-BP, 12.5 mg/mL, purified as described in Lisman, Blood 2006) + laminin (50  $\mu\text{g}/\text{mL}$ , from human plasma); (ii) VWF-BP + laminin + rhodocytin

(250  $\mu\text{g}/\text{mL}$ , from BioSource and purified as described in Hooley, Biochemistry 2008); (iii) collagen type I (100  $\mu\text{g}/\text{mL}$ , Nycomed Pharma, Munich, Germany). The coated coverslips were blocked with modified Tyrode's Hepes buffer pH 7.45 (TH-buffer: 5 mM Hepes, 136 mM NaCl, 2.7 mM KCl, 2 mM  $\text{MgCl}_2$ , 0.42 mM  $\text{NaH}_2\text{PO}_4$ ) containing 1% bovine serum albumin and mounted into parallel plate flow chambers.

#### *Platelet flow adhesion*

Blood was collected as above into 40  $\mu\text{M}$  PPACK, 5 units (U)/mL heparin and 50 U/mL fragmin (final concentrations) and perfused for 3.5 minutes, at a wall-shear rate of  $1000\text{ s}^{-1}$ , over glass coverslips coated with microspots of indicated platelet agonists.<sup>6</sup> Images were captured with an EVOS microscope (Life Technologies, Carlsbad, CA, USA) and analyzed using Fiji (Figure S7).<sup>7</sup>

#### *Platelet flow adhesion image capture and analysis*

Immediately after perfusion of blood was complete, brightfield images were captured from each microspot. Thrombi were then stained using TH-buffer containing 1 mg/mL glucose and 1 mg/mL bovine serum albumin, supplemented with 2 mM  $\text{CaCl}_2$ , 1 U/mL heparin, Alexa647-conjugated annexin A5 (1:200, Invitrogen Life Technologies, Carlsbad, CA, USA), FITC-conjugated anti-P-selectin antibody (1:40) and PE-conjugated anti-JON/A antibody (1:20). Per microspot, 2 (brightfield) or 3 (fluorescence) representative images were taken and analyzed.

Recorded images were analyzed using semi-automated scripts written in Fiji software (Laboratory for Optical and Computational Instrumentation at the University of Wisconsin-Madison, USA). This resulted in percentages of surface area coverage (%SAC) of deposited platelets/thrombus (from brightfield images), and of %SAC of platelet/thrombus fluorescence per fluorescent label. In addition, brightfield images

were analyzed for a morphological score (scale 0-5), thrombus contraction score (scale 0-3) and thrombus height (multilayer, scale 0-3) in comparison to reference images, to provide an indication of the overall size and height of platelet aggregates on the microspots (Figure S7, De Witt, Nat Comm 2014). Finally, the %SAC of multilayered thrombi was analyzed by manual coloring in Fiji.

#### *Platelet biochemistry*

All stimulations were conducted in the presence of 10  $\mu$ M Iotrafiban, 37°C with constant stirring at 1,200 rpm. Whole cell lysates were prepared, immunoprecipitations performed and resolved by SDS-PAGE, as previously described,<sup>8</sup> using washed platelets at  $4\text{-}5 \times 10^8/\text{mL}$ . Band intensities were quantified using ImageJ and normalized to reblots of either pan-Syk or tubulin as stated in Figure Legends.

#### *Protein production for structural analysis of G6b-B-Shp2 interaction*

Human G6b-B p-ITIM (residues 206-215; EPSLL[pY]ADLD), p-ITSM (residues 232-241; DASTI[pY]AVVV) and dual p-ITIM/p-ITSM (residues 206-241; EPSLL[pY]ADLDHLALSRPRRLSTADPADASTI[pY]AVVV) peptides were synthesized by Alta Bioscience (Birmingham, UK) or Genscript (NJ, USA). All peptides were N-terminally acetylated, while only p-ITIM was C-terminally amidated. The individual human SH2 domain constructs were provided by Tony Pawson (University of Toronto). The tandem SH2 domain construct containing residues 4-216 of wild-type Shp2, preceded by a TEV protease cleavable poly-histidine tag, was inserted into a pNIC28-Bsa4 vector obtained from SGC (Oxford, UK) by ligation independent cloning. Proteins were expressed in E. coli using minimal M9 media with  $^{15}\text{NH}_4\text{Cl}$  as the sole nitrogen source and, for assignment purposes, uniformly labeled  $^{13}\text{C}$ -

glucose as the sole carbon source. Proteins were purified using Ni-NTA affinity columns followed by size exclusion chromatography.

### *Structural analysis of G6b-B-Shp2 interaction*

NMR spectroscopy was performed at 25°C using a 600 MHz Varian Direct Drive spectrometer for the individual SH2 domains and an 800 MHz Varian Inova spectrometer for the tandem SH2 constructs. Protein concentrations for all titrations were 400 µM. Spectra were processed using NMRpipe,<sup>9</sup> and analyzed using CCPN analysis.<sup>10</sup> Model structures of tandem SH2 binding to the phosphorylated C-terminal tail of G6b-B were generated using HADDOCK.<sup>11,12</sup>

For residue-specific NMR assignments either BEST (Lescop et al. 2007) (for the individual SH2 domains) or standard versions (for the tandem SH2) of HNCOCA, HNCA, HNCO, HNCACO, HNCACB and HNCOCACB spectra were obtained.

Titration data were collected using SOFAST-HMQC experiments (Schanda et al. 2005).

For model structures the pdb file 5DF6 (Liu et al. 2016) was used as the template for the protein structure. Binding of the peptide to the protein was assumed to be canonical with respect to the pY pocket. Distance restraints of 7Å between R128-CZ: pY237-P and R32-CZ:pY211-P were used to orientate the peptide with nSH2 binding to ITIM and cSH2 binding to ITSM. Peptide residues outside the canonical SH2 domain recognition site (pY, +1, +3) were allowed to be fully flexible during the HADDOCK calculation as were the residues linking the two SH2 domains (102-110). Initial peptide complex structure generation and model visualization was performed using PyMOL (Schrödinger, Cambridge, UK).

## **References**



1. Mazharian A, Wang YJ, Mori J, et al. Mice lacking the ITIM-containing receptor G6b-B exhibit macrothrombocytopenia and aberrant platelet function. *Sci Signal*. 2012;5(248):ra78.
2. Senis YA, Atkinson BT, Pearce AC, et al. Role of the p110delta PI 3-kinase in integrin and ITAM receptor signalling in platelets. *Platelets*. 2005;16(3-4):191-202.
3. McCarty OJ, Larson MK, Auger JM, et al. Rac1 is essential for platelet lamellipodia formation and aggregate stability under flow. *J Biol Chem*. 2005;280(47):39474-39484.
4. Senis YA, Tomlinson MG, Ellison S, et al. The tyrosine phosphatase CD148 is an essential positive regulator of platelet activation and thrombosis. *Blood*. 2009;113(20):4942-4954.
5. Ohlmann P, Eckly A, Freund M, Cazenave JP, Offermanns S, Gachet C. ADP induces partial platelet aggregation without shape change and potentiates collagen-induced aggregation in the absence of Galphaq. *Blood*. 2000;96(6):2134-2139.
6. de Witt SM, Swieringa F, Cavill R, et al. Identification of platelet function defects by multi-parameter assessment of thrombus formation. *Nature Communications*. 2014;5.
7. Schindelin J, Arganda-Carreras I, Frise E, et al. Fiji: an open-source platform for biological-image analysis. *Nat Methods*. 2012;9(7):676-682.
8. Pearce AC, Senis YA, Billadeau DD, Turner M, Watson SP, Vigorito E. Vav1 and vav3 have critical but redundant roles in mediating platelet activation by collagen. *J Biol Chem*. 2004;279(52):53955-53962.
9. Delaglio F, Grzesiek S, Vuister GW, Zhu G, Pfeifer J, Bax A. NMRPipe: a multidimensional spectral processing system based on UNIX pipes. *J Biomol NMR*. 1995;6(3):277-293.
10. Vranken WF, Boucher W, Stevens TJ, et al. The CCPN data model for NMR spectroscopy: development of a software pipeline. *Proteins*. 2005;59(4):687-696.
11. van Zundert GC, Rodrigues JP, Trellet M, et al. The HADDOCK2.2 Web Server: User-Friendly Integrative Modeling of Biomolecular Complexes. *J Mol Biol*. 2016;428(4):720-725.
12. Wassenaar TA, de Vries S, Bonvin AM, Bekker H. SQUEEZE-E: The Optimal Solution for Molecular Simulations with Periodic Boundary Conditions. *J Chem Theory Comput*. 2012;8(10):3618-3627.

**Table S1. Offspring from het × het breeding pairs**

Genotype	Expected frequency	Observed frequency
<i>WT (G6b<sup>+/+</sup>)</i>	25% (60)	29% (70)
<i>Heterozygous (G6b<sup>+/diYF</sup>)</i>	50% (121)	46% (111)
<i>Homozygous (G6b<sup>diYF/diYF</sup>)</i>	25% (60)	25% (60)
Total	100% (241)	100% (241)

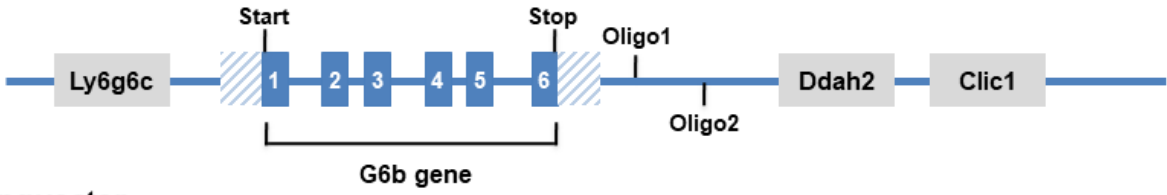
Data was collected from 13 breeding pairs (*G6b<sup>+/diYF</sup>* × *G6b<sup>+/diYF</sup>*) and analysed using  $\chi^2$  test ( $P = 0.2875$ )

**Table S2. Peripheral blood cell counts**

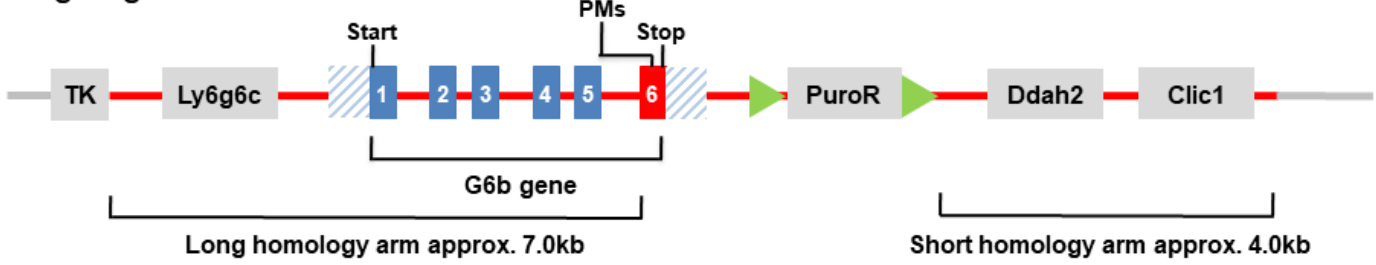
Haematological parameters	<i>WT</i> (mean ± SD, n=24)	<i>G6b-B diY/F</i> (mean ± SD, n=24)
Platelets (10 <sup>9</sup> /L)	1093 ± 230	258 ± 64***
Mean platelet volume (fL)	5.8 ± 0.2	7.9 ± 1.8***
Plateletcrit (%)	0.41 ± 0.10	0.10 ± 0.06***
Red blood cells (10 <sup>12</sup> /L)	10.9 ± 0.6	10.4 ± 1.1
Hematocrit (%)	31.8 ± 2.6	29.4 ± 3.7*
White blood cells (10 <sup>9</sup> /L)	8.3 ± 4.6	9.8 ± 4.3
Lymphocytes (10 <sup>9</sup> /L)	5.5 ± 3.4	12.5 ± 4.6***
Monocytes (10 <sup>9</sup> /L)	0.70 ± 0.60	0.90 ± 0.60
Neutrophils (10 <sup>9</sup> /L)	0.65 ± 0.45	1.10 ± 0.76*
Eosinophils (10 <sup>9</sup> /L)	0.01 ± 0.04	0.00 ± 0.04
Basophils (10 <sup>9</sup> /L)	0.39 ± 1.39	0.10 ± 0.27

\* indicates  $P < 0.05$  and \*\*\* indicates  $P < 0.001$  with Students t-test

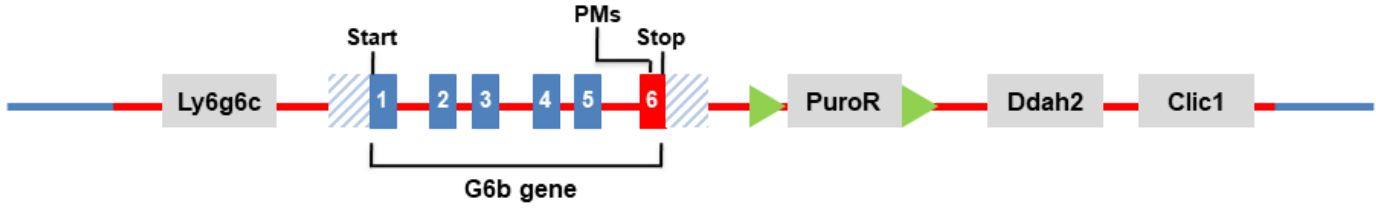
**A Mouse genomic locus**



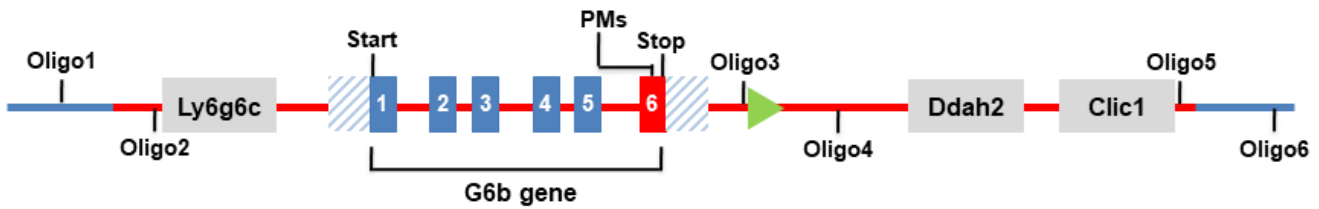
**B Targeting vector**



**C Targeted allele (after homologous recombination)**



**D Constitutive KI allele (after Flp recombination)**



	G6b exon		G6b untranslated region		Mutated G6b exon		Neighbouring gene
	Mouse genomic region		Vector knock-in region		Vector region		
	Flippase recognition target	PMs	Point mutations	Oligo	PCR primer target		
	Start	Start codon		Stop	Stop codon		

**Figure S1. Targeting strategy for constitutive knock-in of *G6b-B diY/F* allele.** A constitutive knock-in strategy was used by Taconic to insert a mutated *G6b* allele into (A) the genomic locus of mouse *G6b*. (B) A targeting vector containing point mutations within exon 6 and a puromycin resistance cassette flanked by Flp recombinase sites was produced. (C) The two homology arms of the targeting vector flanking the mutated exon 6 provided sites for homologous recombination to insert the mutated gene into the C57BL/6NTac embryonic stem cell genome. (D) The puromycin resistance was removed by crossing mice expressing the *G6b-B diY/F* allele with a Flpe recombinase expressing mouse producing the final constitutive knock-in allele.

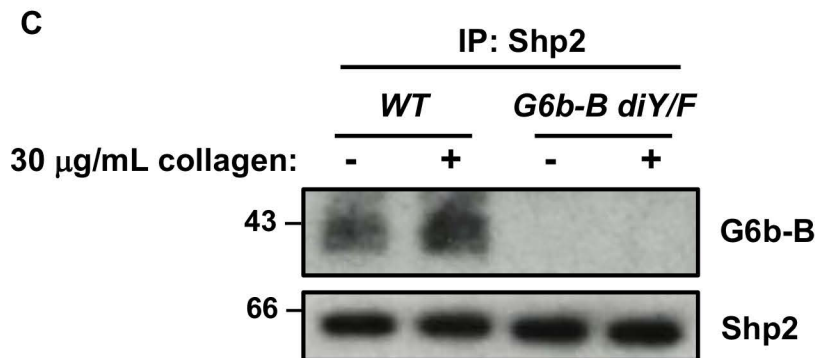
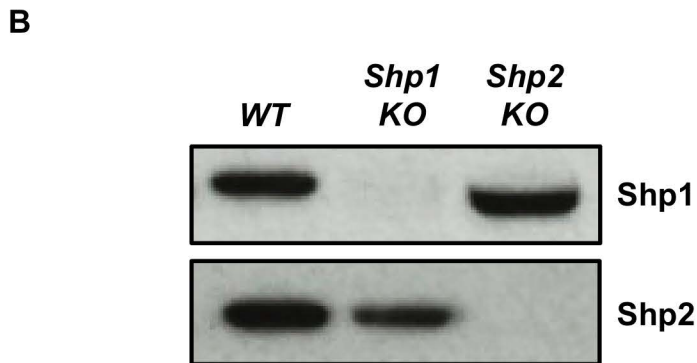
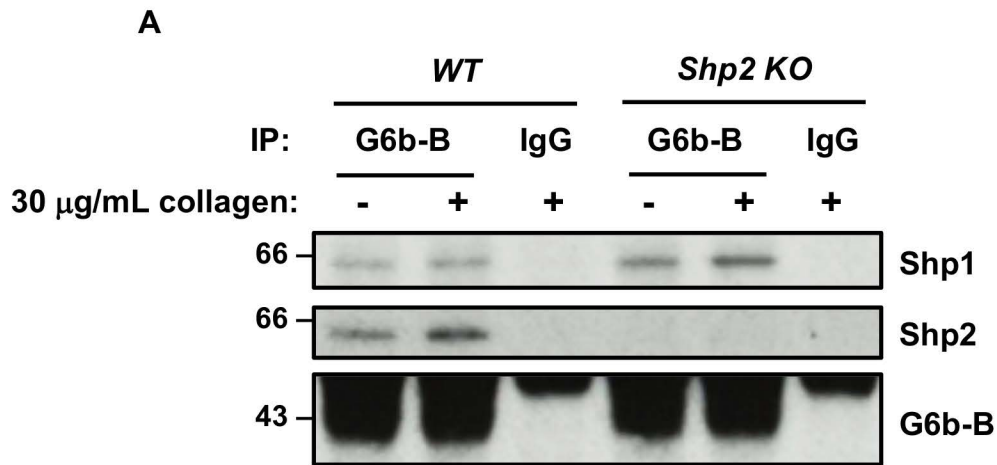
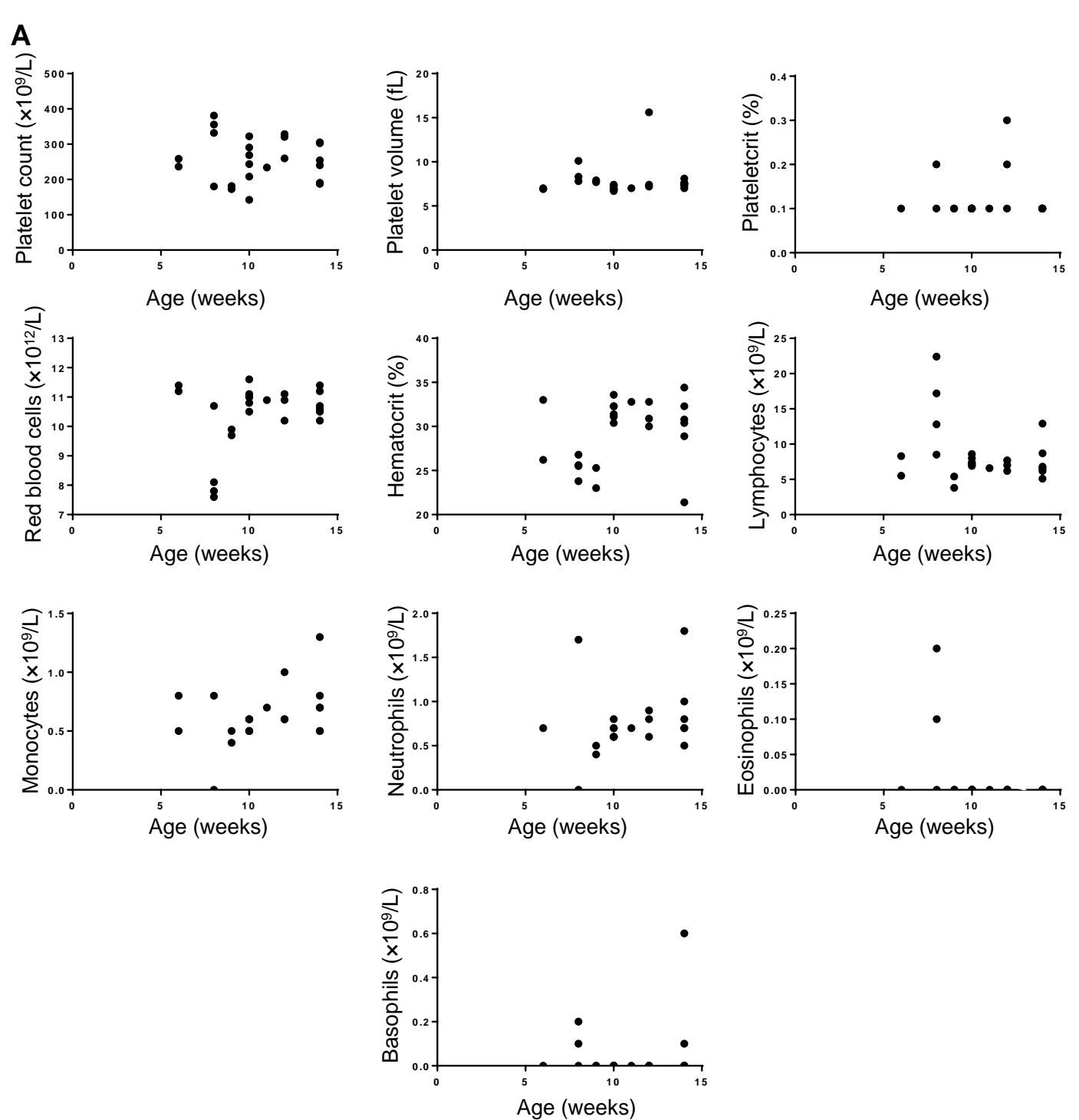


**Figure S2. Interaction of G6b-B with Shp1 and Shp2.** (A) Immunoprecipitation of G6b-B in *WT* and *Shp2 KO* mouse washed platelets ( $4 \times 10^8$ /mL) was performed to investigate the specificity of Shp1 and Shp2 antibodies. (B) Specificity of Shp1 and Shp2 antibodies were also investigated in whole cell lysates from *WT*, *Shp1 KO* and *Shp2 KO* mouse platelets. (C) Basal and 30  $\mu$ g/mL collagen activated platelets were lysed and Shp2 immunoprecipitated to investigate the co-immunoprecipitation of G6b-B. Representative blots from two independent experiments.



**B**

	Platelet count	Platelet volume	Plateletcrit	Red blood cells	Hematocrit	Lymphocytes	Monocytes	Neutrophils	Eosinophils	Basophils
R <sup>2</sup>	0.00	0.00	0.01	0.09	0.08	0.07	0.21	0.12	0.13	0.02
P-value	0.80	0.13	0.63	0.15	0.18	0.22	0.02	0.10	0.09	0.49

**Figure S3. Blood cell counts variation is independent of age in *G6b-B diY/F* mice.** (A) Blood cell counts were plotted against age for *G6b-B diY/F* mice (n=24). (B) Regression analysis indicates that there is no correlation between age and hematological parameters.

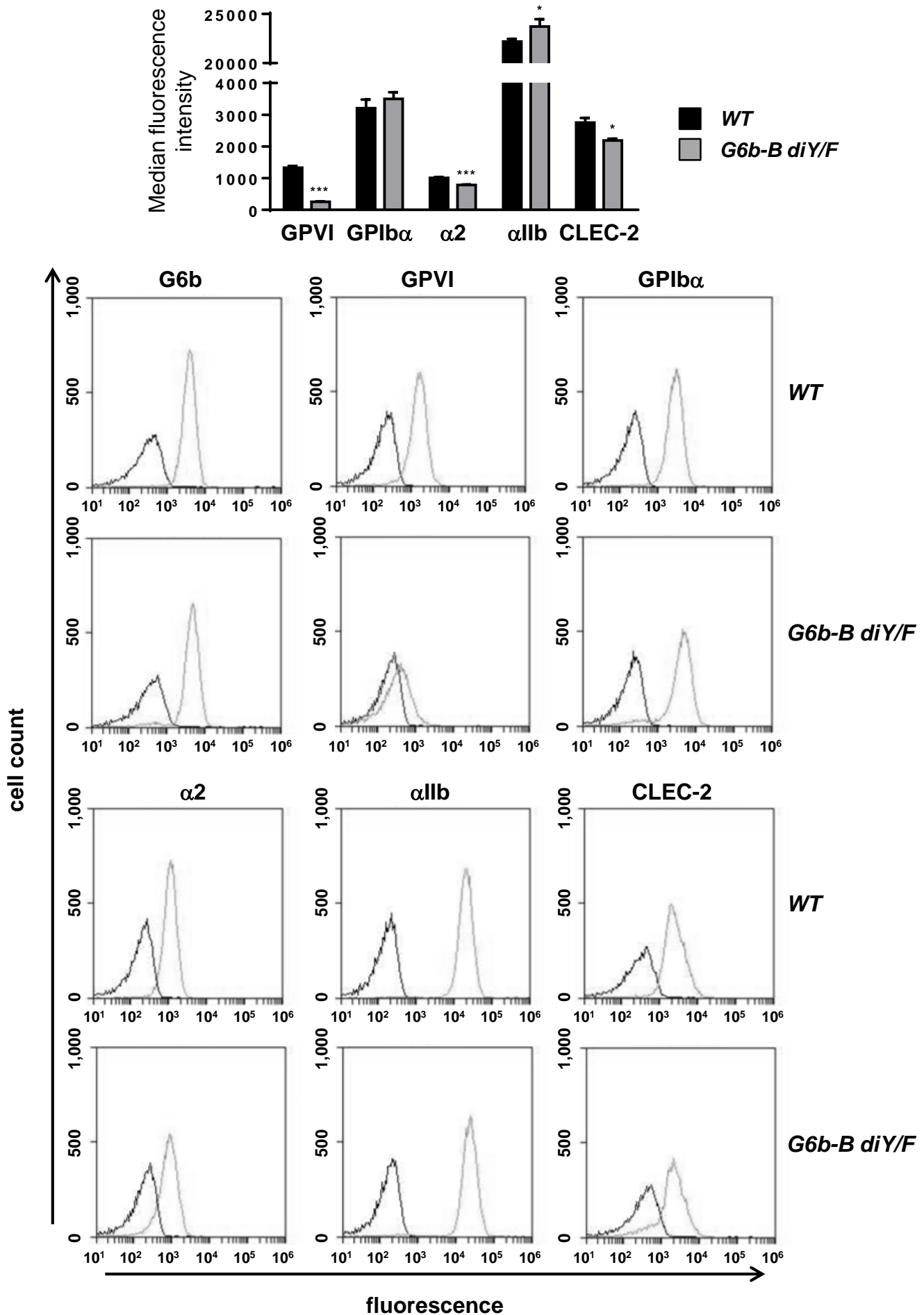


**Figure S4. Quantification of surface receptor expression.** (A) Median fluorescence intensity (mean  $\pm$  SEM,  $n=5-6$ , \*  $P<0.05$ , \*\*\*  $P<0.001$ ). (B) Representative histograms. IgG control (dark grey) and respective staining (light grey).

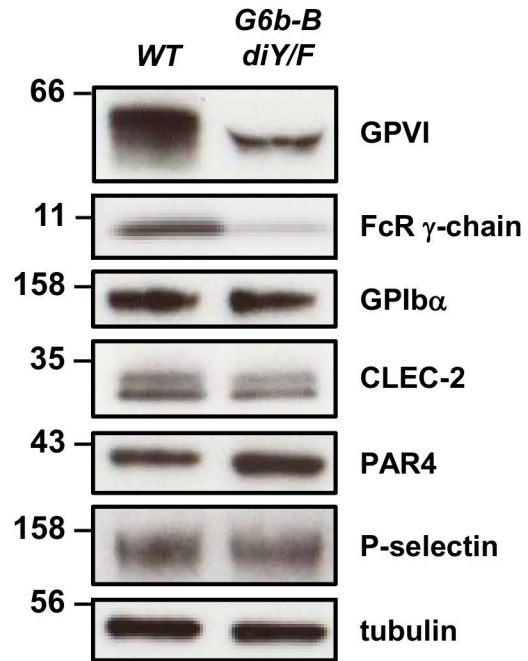


**Figure S5. Total protein expression levels.** Lysates were prepared from washed platelets ( $4 \times 10^8/\text{mL}$ ).

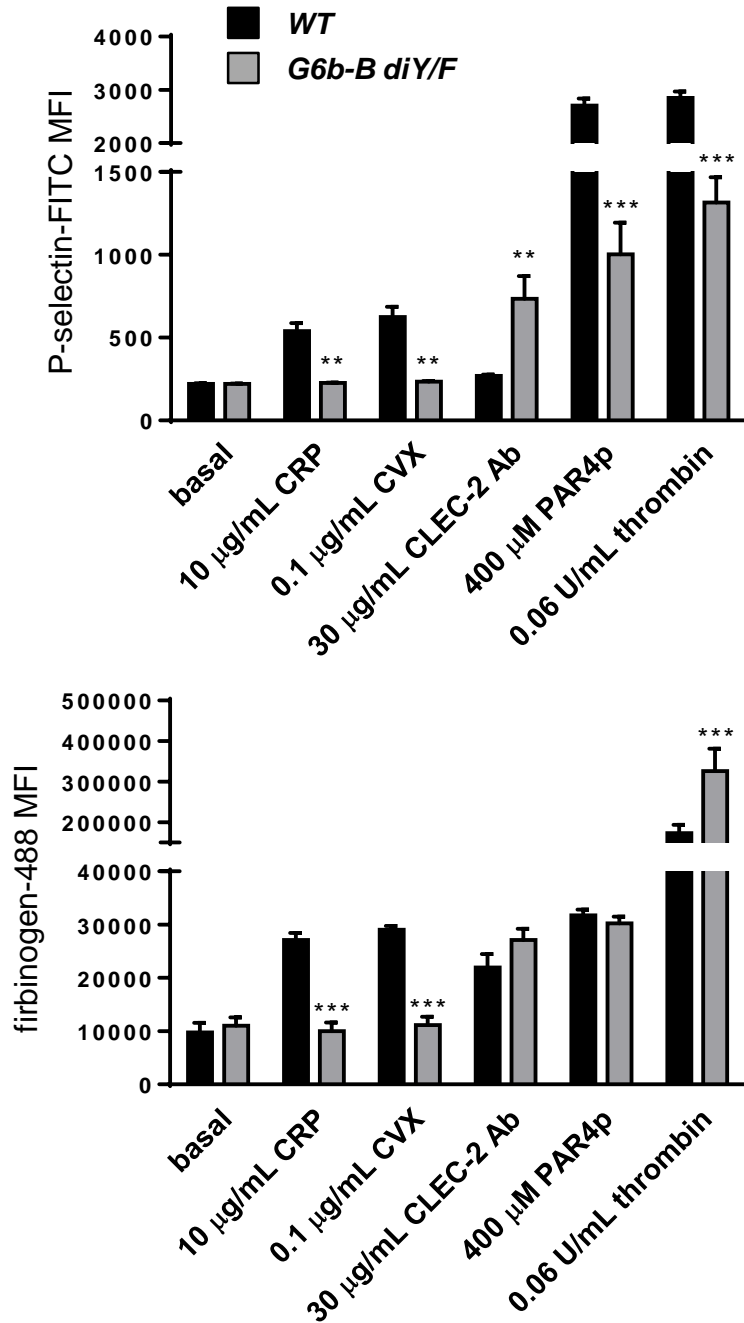


**Figure S6. P-selectin exposure and fibrinogen binding in washed platelets.** (A) anti-P-selectin-FITC and (B) fibrinogen-488 binding to washed platelets ( $2 \times 10^7$ /mL) following stimulation with the indicated agonists. Mean  $\pm$  SEM,  $n=5$ , \*\*  $P<0.01$ , \*\*\*  $P<0.0001$ .



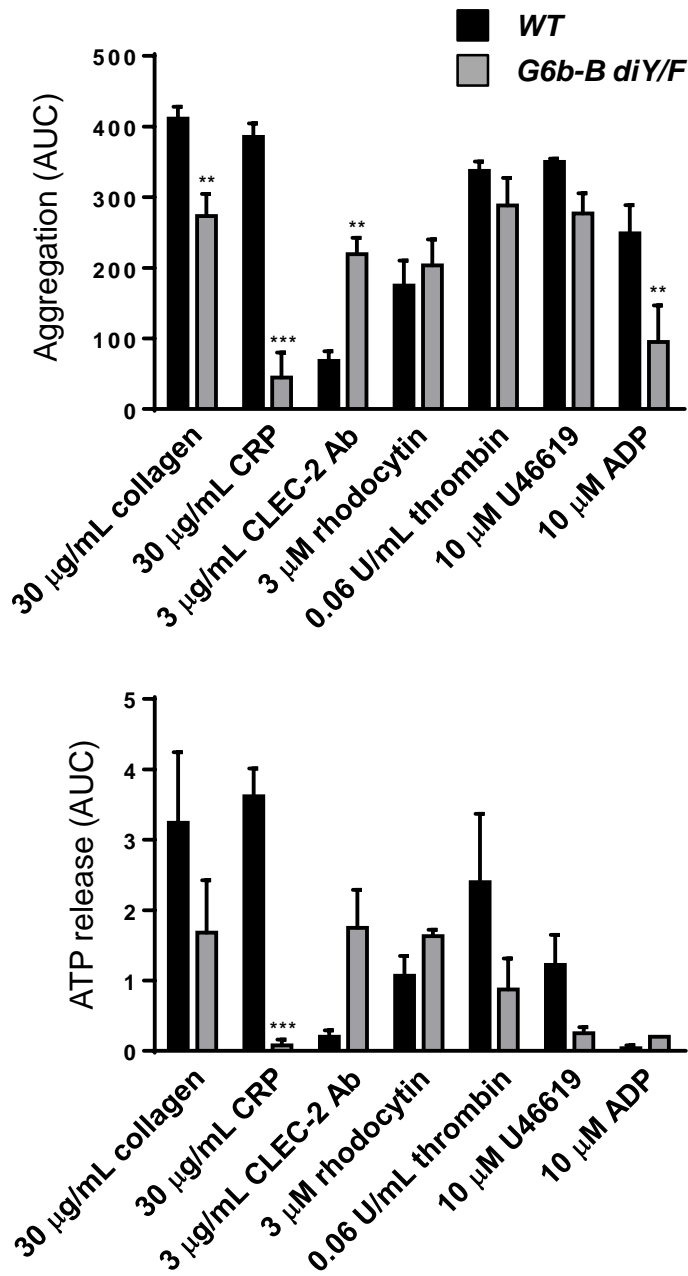
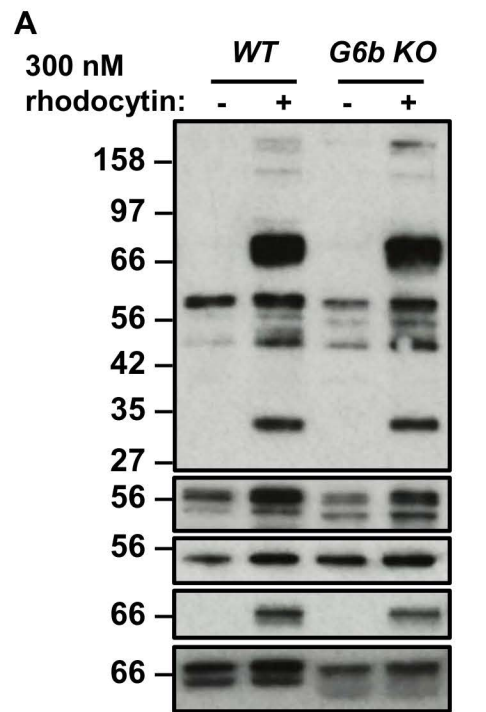
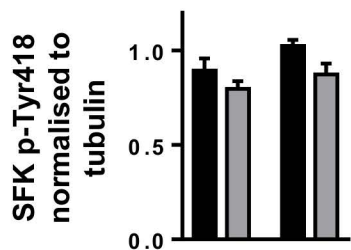


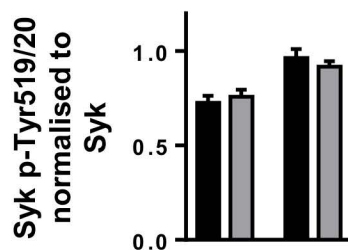
**Figure S7. Analysis of aggregation and ATP release.** Washed platelets ( $2 \times 10^8$ /mL) were activated with the indicated agonists in a lumi-aggregometer. For ADP stimulations platelets were washed in the presence of 0.02 U/mL apyrase and once prepared supplemented with 1  $\mu$ M  $\text{CaCl}_2$  and 50  $\mu$ g/ml fibrinogen. Area under the curve (AUC) of aggregation and ATP release was analysed, mean  $\pm$  SEM,  $n=3-5$ , \*\*  $P < 0.01$ , \*\*\*  $P < 0.0001$ .



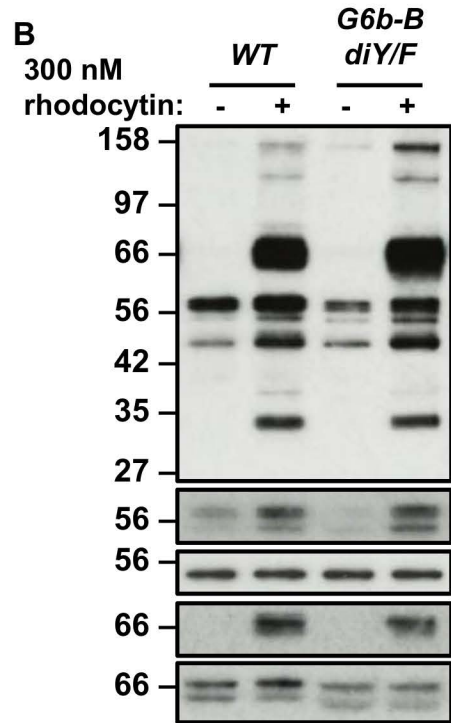
■ WT    □ G6b KO



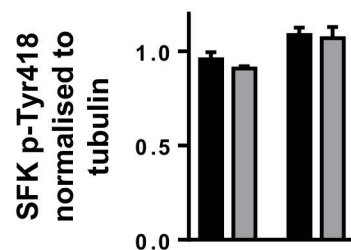
300 nM rhodocytin: - +



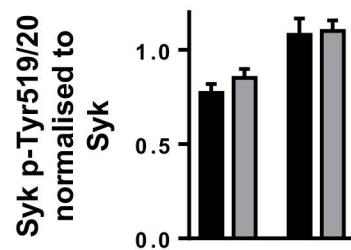
300 nM rhodocytin: - +



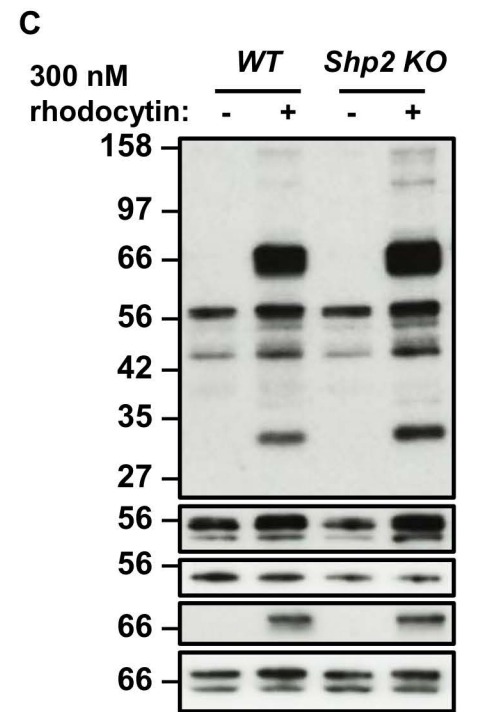
■ WT    □ G6b-B diY/F



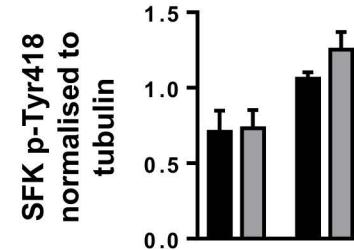
300 nM rhodocytin: - +



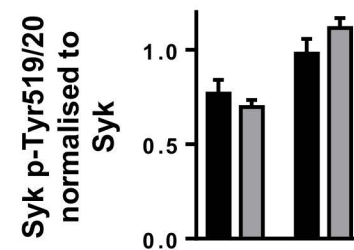
300 nM rhodocytin: - +



■ WT    □ Shp2 KO



300 nM rhodocytin: - +

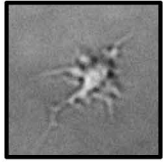


300 nM rhodocytin: - +

**Figure S8. Rhodocytin signalling in *G6b-B diY/F*, *G6b KO* and *Shp2 KO* mouse platelets.** Washed platelets ( $4 \times 10^8/\text{mL}$ ) from indicated genotypes were activated with 300 nM rhodocytin, 3 minutes, 10  $\mu\text{M}$  Itrafiban, 37°C, 1200 rpm stirring. Stimulations were terminated by lysing cells and proteins were resolved by SDS-PAGE to investigate signalling events using the indicated phospho-specific antibodies. Src p-Tyr418 and Syk p-Tyr519/20 were quantified using ImageJ. Representative blots from n=3-4.



**unspread**



**formation of filopodia**

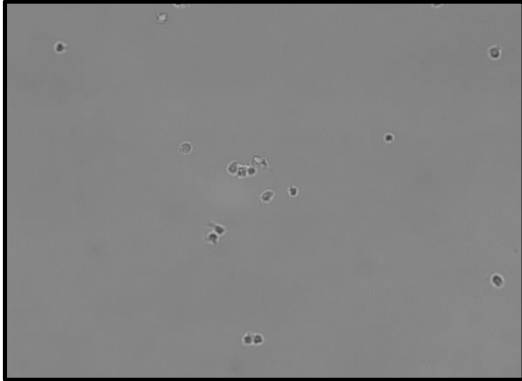


**formation of lamellipodia**

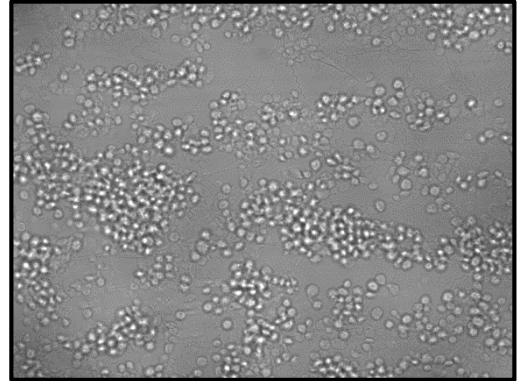


**fully spread**

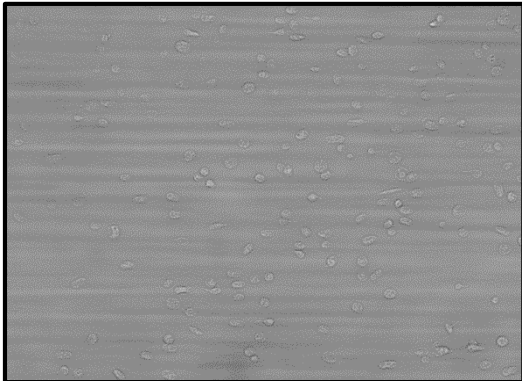
**Figure S9. Platelet spreading on fibrinogen scoring categories**



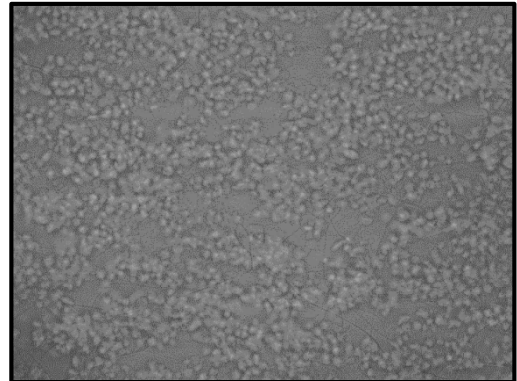
**Morphological score: 0**  
**Contraction score: 0**  
**Multilayer score: 0**



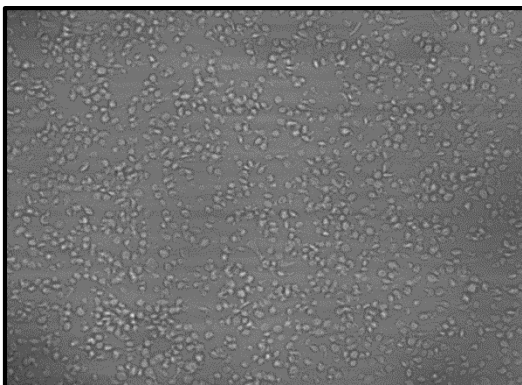
**Morphological score: 3**  
**Contraction score: 1**  
**Multilayer score: 1**



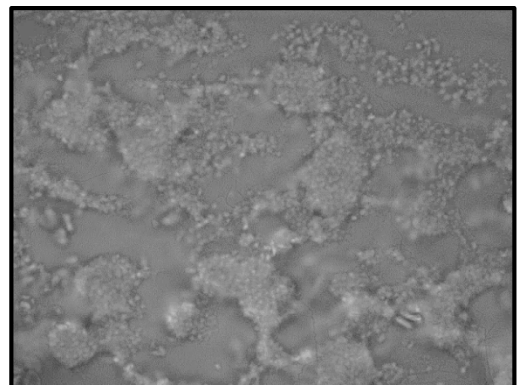
**Morphological score: 1**  
**Contraction score: 0**  
**Multilayer score: 0**



**Morphological score: 4**  
**Contraction score: 2**  
**Multilayer score: 2**



**Morphological score: 2**  
**Contraction score: 0**  
**Multilayer score: 0**



**Morphological score: 5**  
**Contraction score: 3**  
**Multilayer score: 3**

**Figure S10. Platelet flow adhesion morphological scoring representative images**